Serotonin signaling regulates insulin-like peptides for growth, reproduction, and metabolism in the disease vector *Aedes aegypti*

Lin Ling[a,b] and Alexander S. Raikhel[a,b,1]

[a]Department of Entomology, University of California, Riverside, CA 92521; and [b]Institute for Integrative Genome Biology, University of California, Riverside, CA 92521

Contributed by Alexander S. Raikhel, September 6, 2018 (sent for review May 15, 2018; reviewed by Christen Mirth, Michael R. Strand, and Marc Tatar)

Disease-transmitting female mosquitoes require a vertebrate blood meal to produce their eggs. An obligatory hematophagous lifestyle, rapid reproduction, and existence of a large number of transmittable diseases make mosquitoes the world's deadliest animals. Attaining optimal body size and nutritional status is critical for mosquitoes to become reproductively competent and effective disease vectors. We report that blood feeding boosts serotonin concentration and elevates the serotonin receptor Aa5HT2B (*Aedes aegypti* 5-hydroxytryptamine receptor, type 2B) transcript level in the fat-body, an insect analog of the vertebrate liver and adipose tissue. *Aa5HT2B* gene disruption using the CRISPR-Cas9 gene-editing approach led to a decreased body size, postponed development, shortened lifespan, retarded ovarian growth, and dramatically diminished lipid accumulation. Expression of the insulin-like peptide (ILP) genes *ilp2* and *ilp6* was down-regulated while that of *ilp5* and *ilp4* was up-regulated in response to *Aa5HT2B* disruption. CRISPR-Cas9 disruption of *ilp2* or *ilp6* resulted in adverse phenotypes similar to those of *Aa5HT2B* disruption, while *ilp5* CRISPR-Cas9 disruption had exactly the opposite effect on growth and metabolism, with significantly increased body size and elevated lipid stores. Simultaneous CRISPR-Cas9 disruption of *Aa5HT2B* and *ilp5* rescued these phenotypic manifestations. *Aa5HT2B* RNAi silencing rendered *ilp6* insensitive to serotonin treatment in the cultured fat-body, suggesting a regulatory link between Aa5HT2B and ILP6. Moreover, CRISPR-Cas9 *ilp6* disruption affects expression of *ilp-2*, *-5*, and *-4*, pointing out on a possible role of ILP6 as a mediator of the Aa5HT2B action.

CRISPR-Cas9 | serotonin receptor | insulin | body size | metabolism

Mosquitoes are the most dangerous animals on earth, causing hundreds of thousands of deaths and millions of illnesses annually. In addition to the energy derived from larval and sugar diets, hematophagous female mosquitoes require an extraordinarily high amount of energy from vertebrate blood to initiate rapid egg maturation (1). Achieving optimal body size and nutritional status is crucial for mosquitoes to become reproductively competent and effective disease vectors. Therefore, understanding regulatory mechanisms underlying both determination of body size and metabolism is important for the development of novel approaches to control mosquito populations, and thus mosquito-borne diseases.

Despite precise control of adult body size being essential for reproductive capacity, fitness, and survival, the associated mechanisms remain a great puzzle (2, 3). In holometabolous insects, adult body size is fully determined by the end of larval growth (2), and mass is accumulated quickly during juvenile growth to provide the energy reserves required by adults (4). *Drosophila*'s eight insulin-like peptides (DILPs) are used to control body size by coordinating growth and maturation with nutrition and other physiological mechanisms (2). For example, insulin-like peptide 8 (DILP8) is produced by imaginal discs in response to tissue damage and growth perturbation; DILP8 delays pupation by inhibiting ecdysone biosynthesis, ensuring that individuals have completed adequate growth to enter the next developmental stage (5, 6). Although other DILPs promote growth, their specific expression patterns suggest that they might carry out distinct physiological functions (2). In *Drosophila* larvae, *dilps1*, *-2*, *-3*, and *-5* are expressed predominantly in neurosecretory cells (IPCs, insulin producing cells) of the brain; ablation of larval IPCs reduces body size with delayed metamorphosis (7). These DILPs regulate growth by means of the canonical insulin/insulin-like growth factor (IGF) pathway. Single gene mutations in insulin/IGF components have been shown to cause a reduction in growth (8–10). Characterization of how these processes differ among different species is of interest in the study of body-size control in biology and evolution.

Metabolic homeostasis in the organism is maintained by both the central nervous system and hormones (11, 12). Serotonin (5-hydroxytryptamine, 5-HT) is a biogenic amine derived from tryptophan and functions as a neurotransmitter in the brain or as a hormone in the periphery (13). For example, female-specific maxillary palp serotonin is involved in mosquito blood feeding (14), and Malpighian tubule serotonin affects the respiration of female mosquitoes (15). Serotonin has been implicated in regulation of various physiological and behavioral processes by interacting with multiple receptor subtypes (16). In vertebrates, serotonin receptors have been classified into seven main receptor subtypes (termed 5HT1 to -7) (17). In insects, these

Significance

Mosquitoes pose an enormous threat to humans by transmitting numerous dangerous diseases. To become reproductively competent and effective disease vectors, it is crucial for them to achieve optimal body size and nutritional status. Elucidation of these processes in mosquitoes has been hampered by the lack of classic genetics tools. CRISPR-Cas9 disruption of the fat-body–specific serotonin receptor *Aa5HT2B* impairs body growth and lipid accumulation in *Aedes aegypti* mosquitoes, the vectors of dengue fever, yellow fever, and Zika virus. Aa5HT2B controls insulin-like peptides. Using the CRISPR-Cas9 approach, we have uncovered differential roles of insulin-like peptides in the control of body size and metabolism, and provided a link between blood feeding and the fat-body–specific serotonin signaling.

Author contributions: L.L. and A.S.R. designed research; L.L. performed research; L.L. contributed new reagents/analytic tools; L.L. and A.S.R. analyzed data; and L.L. and A.S.R. wrote the paper.

Reviewers: C.M., Monash University; M.R.S., University of Georgia; and M.T., Brown University.

The authors declare no conflict of interest.

[1]To whom correspondence should be addressed. Email: alexander.raikhel@ucr.edu.

This article contains supporting information online at www.pnas.org/lookup/suppl/doi:10.1073/pnas.1808243115/-/DCSupplemental.

Published online October 1, 2018.

receptors are also wildly distributed and are classified based on sequence similarities to those in vertebrates (16). Thus, characterization of the role of serotonin receptors may deepen our understanding of mosquito metabolism and growth.

The insect fat-body, an analog of vertebrate liver and adipose tissue, is a target for hormones and has a changing metabolic role in accordance with insect development (18). It is the principal tissue for intermediary metabolism, immunity, and production of yolk protein precursors during reproduction (19). However, the mechanisms of serotonin action specific to the fat-body are poorly understood.

In this study, we used the CRISPR-Cas9 gene-editing approach to investigate mechanisms determining body size and metabolism in *Aedes aegypti* mosquitoes. We demonstrated that the fat-body–specific serotonin receptor Aa5HT2B (*Aedes aegypti* 5-hydroxytryptamine receptor, type 2B) plays a key role in these processes, and its action is mediated by ILP6, which in turn regulates expression of *ilp2*, *-5*, and *-4*. Use of this CRISPR-Cas9 approach has uncovered differential roles of ILPs in body size determination and metabolism in *A. aegypti*.

Results

Blood Feeding Boosts Serotonin in Mosquito Periphery and Increases Serotonin Receptor Aa5HT2B Level in the Fat-Body. Female mosquitoes are not capable of developing eggs until they change their diet from carbohydrate-rich nectar to vertebrate blood, which contains nearly 80% protein (20). To examine whether serotonin levels are affected by the diet switch, we investigated the distribution of serotonin in the head and peripheral tissues in both sugar-fed and blood-fed females. After a blood meal, the serotonin level increased in peripheral tissues but was not significantly changed in the head (Fig. 1*A*). Phylogenetic analysis utilizing ORF amino acid sequences of *Drosophila melanogaster* and *A. aegypti* serotonin receptors was performed using the maximum-likelihood method (21). This analysis and sequence alignment distinguished five serotonin receptor

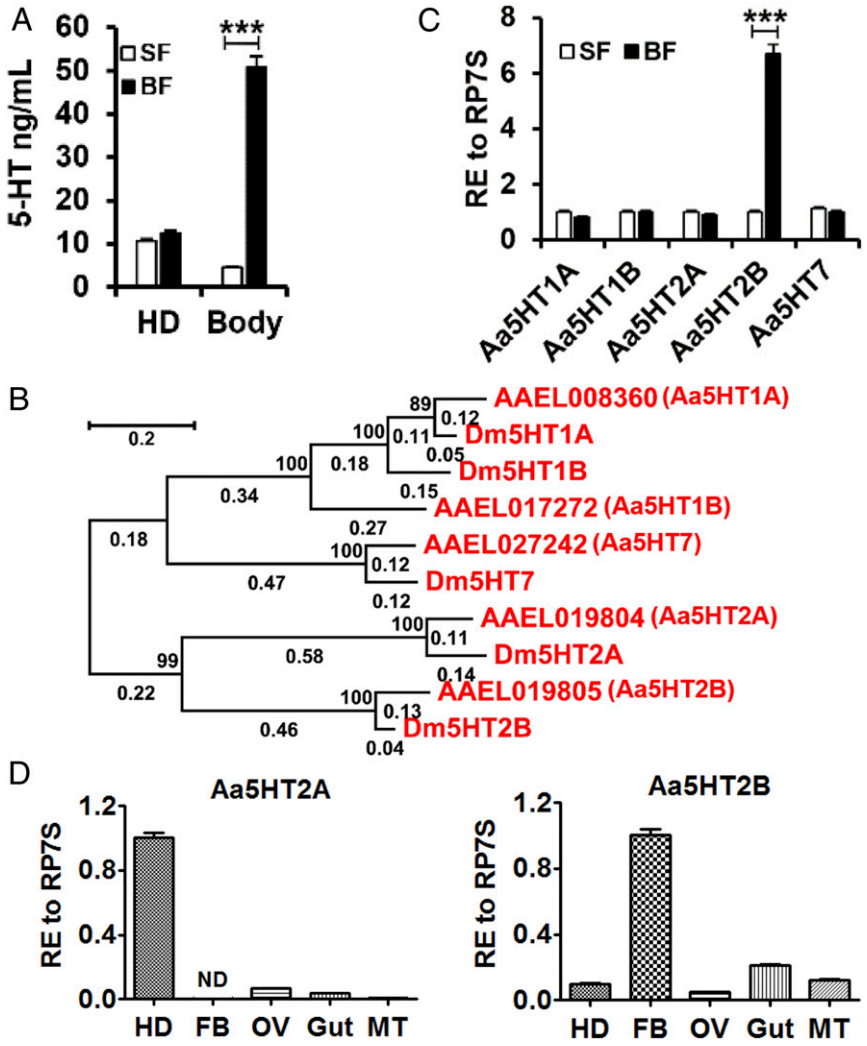

Fig. 1. Characterization of serotonin and serotonin receptors in the mosquito *A. aegypti*. (*A*) Blood feeding elevates the amount of serotonin in the periphery but not the head of female mosquitoes. (*B*) Phylogenetic tree, branch lengths and bootstrap values of serotonin receptors of *D. melanogaster* and *A. aegypti*. The numbers above the branches represent the bootstrap values for each branch (2,000 replications, significantly support for the related sequences common to a node). Branch lengths are scaled (shown by the numbers below the branches) and indicate the number of substitutions per site. (Scale bar indicates 0.2 units of branch length.) (*C*) The relative expression (RE) of serotonin receptor *Aa5HT2B* is greater in blood-fed (BF, 24-h PBM) than in sugar-fed (SF) mosquitoes. Whole bodies were used for tests. (*D*) Relative expression of *Aa5HT2A* and *Aa5HT2B* in the head (HD), fat-body (FB), ovaries (OV), gut and Malpighian tubules (MT) in WT female mosquitoes at 24-h PBM. Data represent three biological replicates (10 individuals in each replication for quantitative real-time PCR; 30 individuals in each replication for 5-HT determination) with three technical replicates and are shown as mean ± SEM. ***$P < 0.001$.

DEVELOPMENTAL BIOLOGY

subtypes in *A. aegypti* mosquitoes—including types 1A, 1B, 2A, 2B, and 7—based on the amino acid identity of their seven-transmembrane domains with those of *D. melanogaster* five serotonin receptor subtypes (Fig. 1*B* and *SI Appendix*, Fig. S1). We then determined the expression of serotonin receptors in sugar-fed and blood-fed females using quantitative real-time PCR analysis. The results show that the serotonin receptor *Aa5HT2B* transcript was significantly enriched in the fat-body after a blood meal compared with sugar-fed mosquitoes (Fig. 1 *C* and *D*). In contrast, other serotonin receptors were not affected (Fig. 1*C*), and a closely related receptor type 2A was significantly enriched in the head (Fig. 1*D*). These results suggest that the serotonin receptor Aa5HT2B may play an important role in altering metabolism in the fat-body to cope with the diet transition.

CRISPR-Cas9 Gene-Editing Disruption of the Receptor *Aa5HT2B* Gene Causes Severe Reduction in Body Size, Lipid Deposition, and Ovary Development. To further investigate the role of Aa5HT2B in mosquitoes, we generated a genomic disruption of the *Aa5HT2B* gene using the CRISPR-Cas9 system. Two specific single-guide RNAs (sgRNAs) were designed, aimed at two sites (T1 and T2) between the cytoplasmic ends of the fifth and the sixth transmembrane domains in the last exon of *Aa5HT2B*, where the receptor C terminus is located to transmit serotonin signals. These sgRNAs were injected into embryos separately, each mixed with Cas9 protein to generate two independent CRISPR-Cas9 *Aa5HT2B* lines. We identified successful genomic disruptions by means of Sanger sequencing in both mosquito lines (Fig. 2*A* and *SI Appendix*, Fig. S2*A*).

To evaluate the impact of *Aa5HT2B* CRISPR-Cas9 disruptions, *Aa5HT2B* mutants (*ΔAa5HT2B-T1* and *-T2*) and WT control mosquitoes were raised and maintained under identical conditions at every stage of their development. For the T1 mutated site, 40% of injected embryos survived, reaching larval stage and further developing into adults with a normal sex ratio (females to males, 210:195). Wing length is the most common and readily available measure of body size (22) and, using this estimate, we found adult size was smaller in 80% of the mutants (Fig. 2*B* and *SI Appendix*, Fig. S2*B*). *ΔAa5HT2B-T1* mutants also exhibited a smaller larval and pupal size (Fig. 2*C* and *SI Appendix*, Fig. S2*C*). We dissected the *ΔAa5HT2B-T1* adult females at 24-h postblood meal (PBM) to evaluate the ovarian development and found that all of those with a reduced body size displayed less ovarian development (*SI Appendix*, Fig. S2*D*). To evaluate the effect of Aa5HT2B in regulating metabolism, we stained the lipid droplets in fat-bodies of CRISPR-Cas9 mutants with Nile red and found them to be considerably smaller at 24 h in PBM adults and fifth-day larvae (wandering last-instar larval stage) than those in the WT controls (Fig. 2*D*). In addition, we measured triacylglycerides (TAG) and glycogen levels in *ΔAa5HT2B-T1* mutants and WT controls, and found that while lipid stores were dramatically lower in *ΔAa5HT2B* mutants, glycogen exhibited the opposite trend, being significantly higher than in WT controls (Fig. 2*E*). The *ΔAa5HT2B-T2* mutant showed a similar phenotype (*SI Appendix*, Figs. S2 *D–G* and S3). Taken together, the *Aa5HT2B* mutants generated using the CRISPR-Cas9 gene-editing approach highlight a critical role of this serotonin receptor, Aa5HT2B, in determination of body size, metabolism, and ovary development.

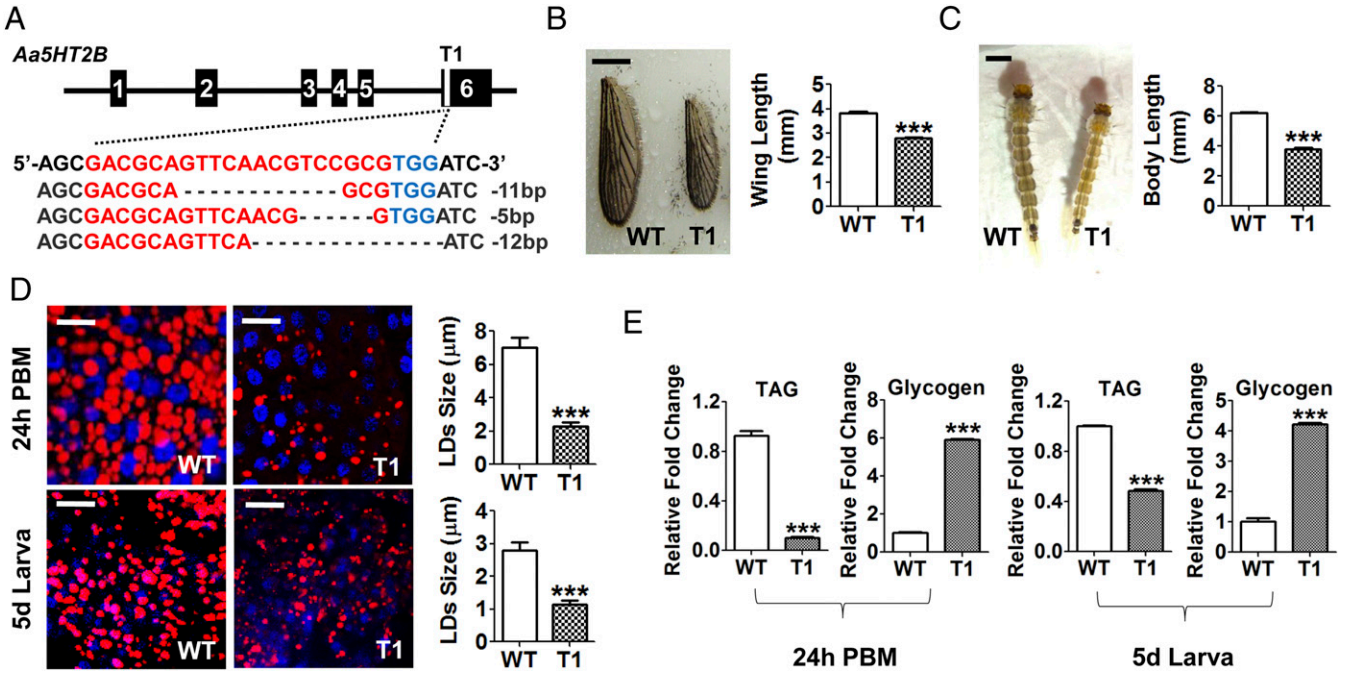

Fig. 2. Genomic disruption of *Aa5HT2B* by CRISPR-Cas9 resulted in a reduced body size and diminished lipid storage. (*A*) Sequence alignment of a sgRNA-targeted (named T1) genomic region. Exons are shown in black boxes. The sequence of the sgRNA target site (labeled in red) is in the last exon, where the receptor C terminus is located to transmit serotonin signals. The protospacer adjacent motif (PAM) sequence is in blue. (*B*) Comparison of wing length of WT control and *ΔAa5HT2B-T1* mutant adults. (Scale bar, 1 mm.) (*C*) *ΔAa5HT2B-T1* larvae also exhibit reduced body length. (Scale bar, 1 mm.) Shown are the last-instar larvae on the fifth day after egg hatching (wandering fourth-instar larval stage). All surviving individuals were used for measurements. (*D*) Lipid droplets in the fat-bodies dissected from WT and *T1* mutant adults and larvae (with reduced body size) at 24-h PBM and the fifth day after egg hatching were detected by Nile red staining and visualized under a Leica SP5 confocal microscope. (Scale bars, 25 μm.) Blue, nuclear staining with DAPI. The lipid droplet sizes (LDs) are significantly lower in *T1* mutant females than in WT. (*E*) TAG levels are significantly less and the glycogen levels significantly higher in *T1* mutant females than in WT. Data represent three biological replicates (six individuals in each replication for LDs, TAG, and glycogen measurement) with three technical replicates and are shown as mean ± SEM. ***$P < 0.001$.

Aa5HT2B Modulates *ilp2*, *-4*, *-5*, and *-6* Gene Expression. A primary focus of fat-body-regulated growth is the insulin signaling pathway, which coordinates nutrition and systemic growth (4). To identify a potential link between the insulin signaling pathway and the smaller body size created by *Aa5HT2B* CRISPR-Cas9 disruption, we determined mRNA levels of ILPs and the insulin/IGF pathway components using quantitative real-time PCR analysis. *ilp2* and *ilp6* were shown to be transcriptionally down-regulated, while *ilp4* and *ilp5* were up-regulated in *ΔAa5HT2B* female mosquitoes compared with WT controls (Fig. 3). In contrast, other *ilp* genes and insulin/IGF pathway components were not affected (Fig. 3). The T2 *Aa5HT2B*-sgRNA showed a similar change (Fig. 3).

We also performed fat-body–specific GAL4 transcription factor-upstream activation sequence (GAL4-UAS) RNA interference (RNAi) to knock down *Aa5HT2B* in adult female mosquitoes. A UAS responder vector was constructed by incorporating two dsAa5HT2B sequences in reverse orientation separated by a short intron (Fig. 4*A*). The fat-body–specific *Vitellogenin* (*Vg*) promoter-GAL4 driver line was generated previously (23). Importantly, the effects of Aa5HT2B RNAi on transcript levels of *ilp2*, *-6*, *-4*, and *-5* in the generated binary transgenic line *Vg-Gal4/UAS-iAa5HT2B* were similar to those in *ΔAa5HT2B* adults (Fig. 4*B*). The expression of yolk protein precursor genes *Vg* or *Lp* (*Lipophorin*) was not affected in this line (Fig. 4 *B* and *C*). Results also showed defects in ovarian development and changes of energy stores (Fig. 4 *D* and *E*). Body-size analysis was unavailable because this RNAi was activated in adults by the female and fat-body–specific *Vg* gene promoter. This assay has provided additional proof of the crucial role of Aa5HT2B in regulating metabolism in the fat-body, an essential energy source for rapid egg development. Taken together, these results suggest that Aa5HT2B is essential for coordinating mosquito body size with nutritional reserves, likely by modulating levels of some ILPs.

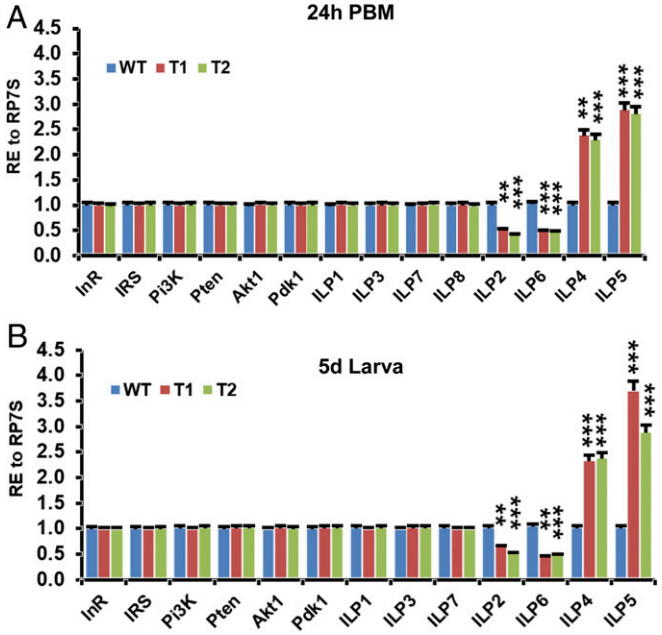

Fig. 3. *ilp2*, *-6*, *-4*, and *-5* are affected by the *Aa5HT2B* CRISPR-Cas9 depletion. (*A*) Expression levels of *ilp2* and *ilp6* transcripts are significantly lower, but those of *ilp4* and *ilp5* are significantly higher in *ΔAa5HT2B* mutant adults (*T1* and *T2* females at 24-h PBM with reduced body size) than WT controls. The expression levels of *ilp1*, *-3*, *-7*, and *-8* and insulin/IGF pathway components are not affected by the depletion of *Aa5HT2B*. (*B*) The *ΔAa5HT2B* mutant larvae (*T1* and *T2* larvae on the fifth day after egg hatching with reduced body size) display the same trend of regulation as adults in transcription. *ilp8* is undetectable in late larvae of WT or mutant females. *Ilp1*, *-3*, *-4*, *-7*, and *8* (head-specific expression) were determined in the head; *ilp6* was determined in the fat-body; other genes were determined in the whole body. Data represent three biological replicates (10 individuals in each replication) with three technical replicates and are shown as mean ± SEM. $^{**}P < 0.01$; $^{***}P < 0.001$.

The Roles of ILPs in Regulation of Body Size. We then investigated functions of ILPs affected by Aa5HT2B. The CRISPR-Cas9 gene-editing system was used to disrupt *ilp2*, *-4*, *-5*, and *-6*. First, we designed the sgRNAs for each of these *ilps* and introduced them individually into embryos ($n = 600$) together with the Cas9 protein. Approximately 22% of embryos injected with *ilp2*-sgRNA, 20% of those with *ilp6*-sgRNA, 36% of those with *ilp5*-sgRNA, and 42% of those with *ilp4*-sgRNA survived, reaching larval stage and adulthood. Insect wings are adult appendages originating from corresponding imaginal disks that develop mostly after the larva has stopped feeding and the body has stopped growing (22). To evaluate the impact of *ilp* disruption on body size, *ilp* CRISPR-Cas9 mutants (*Δilp2*, *Δilp6*, *Δilp5*, *Δilp4*) and WT control animals were raised and maintained under identical conditions at all stages of their development. Body sizes of the last-instar larvae, pupae, and adults were then evaluated. *Δilp2* (44%, 57 of 129) and *Δilp6* (38%, 45 of 118) mosquitoes exhibited smaller body sizes, while *Δilp5* (60%, 129 of 216) mosquitoes exhibited a larger body size than WT controls (Fig. 5*A* and *SI Appendix*, Fig. S4). However, *Δilp4* showed nearly normal body size: that is, similar to WT (Fig. 5*A* and *SI Appendix*, Fig. S4). To ascertain whether wing size is attuned with body size, we measured the wing length of CRISPR-Cas9 mutants and WT female mosquitoes. We found that the wing length corresponded to changes in their body size. Compared with WT control, wing length was shorter in *ΔAa5HT2B* (27%), *Δilp2* (23%), and *Δilp6* (28%), longer in *Δilp5* (21%), but the same as WT in *Δilp4* (Fig. 5*B*). Our DNA sequencing resulted in the successful genomic mutations of the target genes (*SI Appendix*, Fig. S5*A*).

In addition, we measured cell sizes in the wings of mutants and WT controls to understand their relationship to body size and nutrition. In insects, a cell size can be determined by counting the number of wing hairs in a defined area (45 × 45-μm squares, $n = 20$), then calculating the mean cell area (24). We found that the mean cell area was less in *ΔAa5HT2B*, *Δilp2*, and *Δilp6* (47%, 30%, and 44%, respectively), greater in *Δilp5* (47%), but the same in *Δilp4* compared with WT control wings (Fig. 5*C*). These results indicate a strong correlation between cell and body sizes.

Differential Effect of ILPs on Mosquito Metabolism. We performed lipid-droplet Nile red staining of CRISPR-Cas9 mutant and WT females and examined them in 24-h PBM adults and fifth-day last-instar larvae (wandering fourth-instar larval stage). In addition, we measured TAG and glycogen levels. Compared with WT controls, lipid stores in the fat-bodies were dramatically higher in *Δilp5* and *Δilp4* mutants, but lower in *Δilp2* and *Δilp6* mutants (Fig. 6). Glycogen exhibited the opposite trend, being depleted in the fat-body of *Δilp5* and *Δilp4* mutants and highly elevated in that of *Δilp2* and *Δilp6* mutants relative to WT controls (Fig. 6). Hence, experiments with CRISPR-Cas9 *ilp* disruptions have clearly demonstrated differential actions of ILPs, with ILP2 and -6 exhibiting a trend opposite that of ILP5 and -4 in regulation of body size and metabolism. We also evaluated the ovarian development in mutant females at 24-h PBM and found that most of those with abnormal body size displayed altered ovarian development. *Δilp2*, *Δilp5*, and *Δilp4* mutant females showed partially developed ovaries and reduced egg deposition, while *Δilp6* mutants had more severe inhibition of follicle formation and egg deposition (*SI Appendix*, Fig. S5*B*).

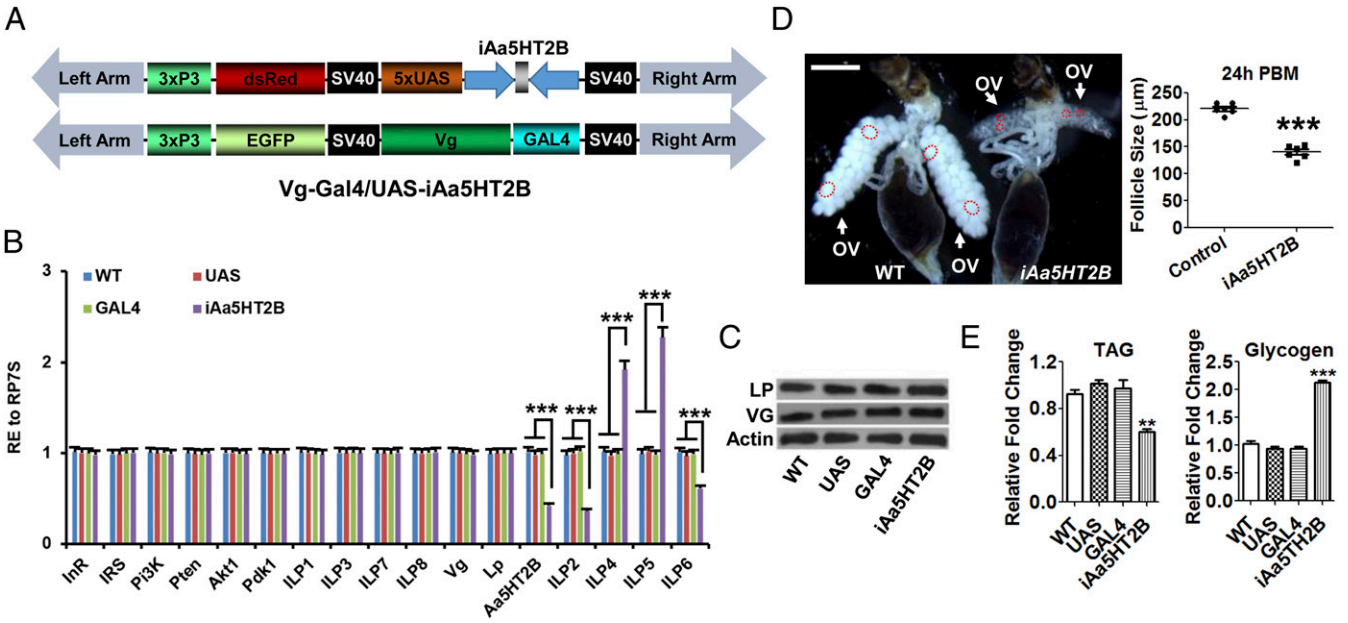

Fig. 4. Fat-body–specific RNAi to knockdown *Aa5HT2B* in female mosquito adults. (*A*) Schematic diagrams of the pBac[3xP3-DsRed, UAS-iAa5HT2B] and pBac [3xP3-EGFP, Vg-Gal4] transgenic vectors. (*B*) The relative expression of *Aa5HT2B*, *ilps*, insulin/IGF pathway components, *Lp* (*Lipophorin*) and *Vg* (*Vitellogenin*) in *Vg-Gal4/UAS-iAa5HT2B* (*iAa5HT2B*) and controls. *iAa5HT2B* displays the same trend of regulation as *ΔAa5HT2B* mutants in these transcripts. *ilp1*, *-3*, *-4*, *-7*, and *-8* (head-specific expression) were determined in the head; *Aa5HT2B* and *ilp6* were determined in the isolated fat-body; other genes were determined in the whole body. (*C*) Western blot showing the normal levels of endogenous yolk protein precursors LP and VG in a transgenic line where the *Vg* promoter was used to drive transgene expression. WT, UAS-responder, and GAL4-driven animals were used as control. (*D*) Comparison of ovaries and follicle sizes in *iAa5HT2B* and WT control. (Scale bar, 1 mm.) The dashed circles show the follicle shape. (*E*) TAG and glycogen levels in *Vg-Gal4/UAS-iAa5HT2B* and controls. *iAa5HT2B* displays the same trend of regulation as *ΔAa5HT2B* mutants in metabolism. Data represent three biological replicates (10 individuals in each replication for qPCR and Western blot assay; six individuals in each replication for TAG and glycogen measurement; six biological replicates with 10 individuals in each replication for follicle size measurement) with three technical replicates and are shown as mean ± SEM. $^{**}P < 0.01$; $^{***}P < 0.001$.

Maturation Time Correlates with Lipid Reserves and Body Size in Response to *Aa5HT2B* or *ilp* CRISPR-Cas9 Disruptions. Mosquitoes can carry over energy reserves from a feeding larval instar stage to a nonfeeding pupal stage, culminating in adult eclosion (22). To identify a link between nutrition reserves, body size, and the timing of maturation, we investigated the percentage of pupation

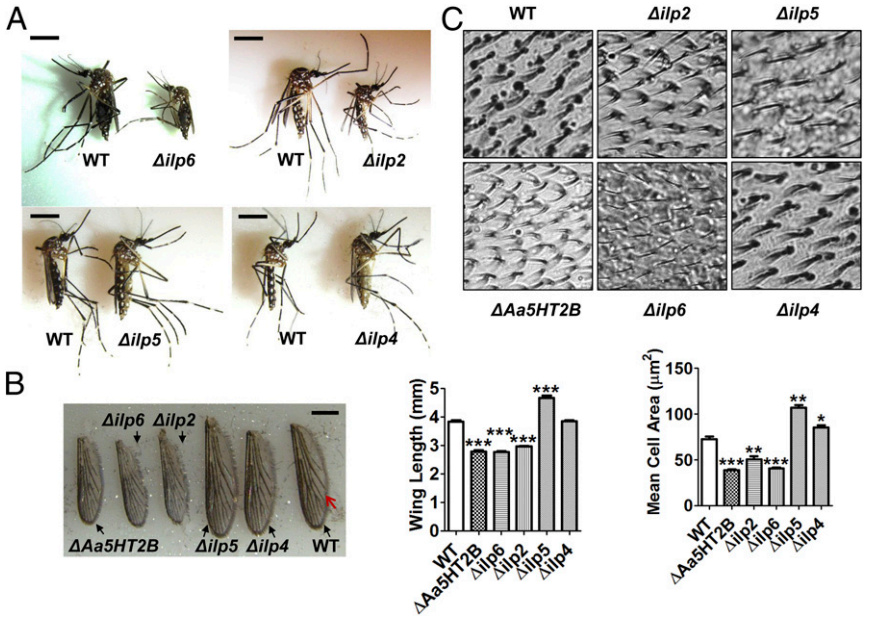

Fig. 5. Body size and wing size variations in *ilp2*, *ilp6*, and *ilp5* CRISPR-Cas9–depleted mosquitoes. (*A*) *Δilp2* and *Δilp6* display smaller body size, but *Δilp5* has a considerably larger body size than WT control. (Scale bars, 2 mm.) (*B*) Comparison of wing length between WT control and mutant females. (Scale bar, 1 mm.) All surviving individuals were used for measurement. (*C*) Mean cell area was determined in the compartment (45 × 45-μm squares, $n = 20$) between two defined veins (indicated by a red arrow in *B*). Data are shown as mean ± SEM. $^{*}P < 0.05$; $^{**}P < 0.01$; $^{***}P < 0.001$.

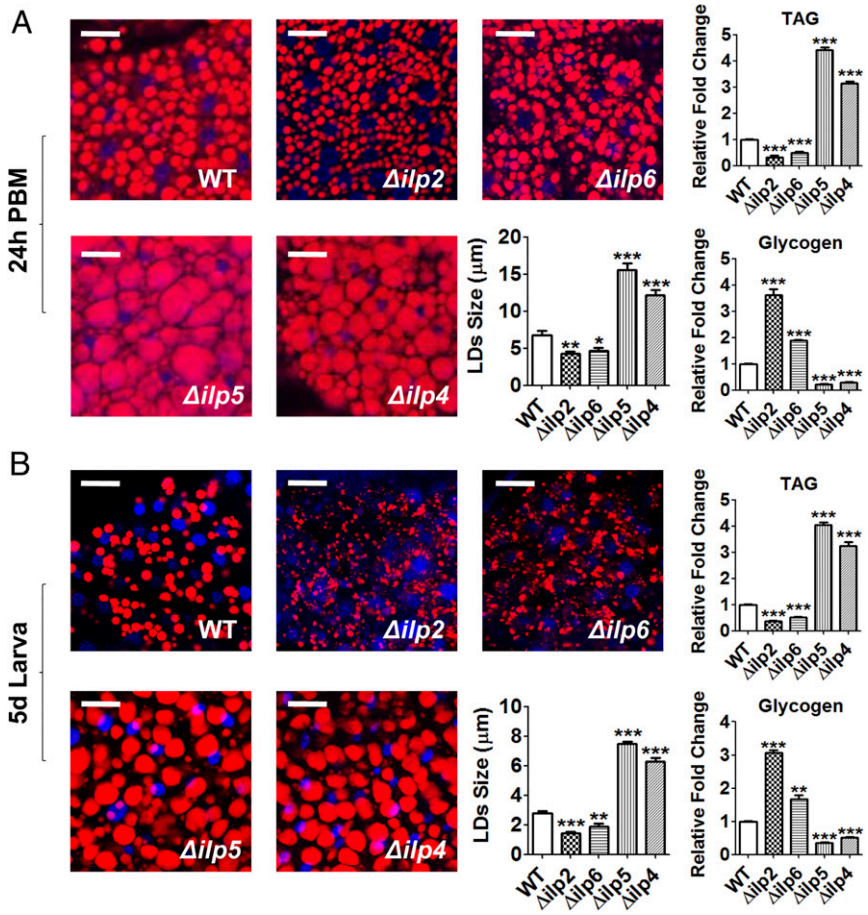

Fig. 6. Lipid and glycogen levels in WT and *ilp* CRISPR-Cas9–depleted mutant females. (*A*) Lipid droplets in the fat-body From WT and *ilp* mutant females (*Δilp2*, *Δilp6*, *Δilp5*, and *Δilp4*) at 24-h PBM were detected using Nile red staining and visualized under a Leica SP5 confocal microscope. (Scale bars, 25 μm.) Blue, DAPI staining. TAG and glycogen levels are affected in mutant females compared with WT control. (*B*) Lipid and glycogen levels in larvae. Fat-bodies were dissected from WT and mutant larvae on the fifth day after hatching. Data represent three biological replicates (six individuals in each replication) with three technical replicates and are shown as mean ± SEM. (Scale bars, 25 μm.) $*P < 0.05$; $**P < 0.01$; $***P < 0.001$.

and eclosion of CRISPR-Cas9 mutants and WT controls. We observed a precocious pupation of mosquitoes with bigger body size and larger lipid stores in *Δilp5* mutants (71% at sixth day and 92% at seventh day), whereas a considerably late pupation occurred in *ΔAa5HT2B* (no pupae at sixth day, 6% at seventh day, and 71% at eighth day), *Δilp2* (no pupae at sixth day, 6% at seventh day, and 73% at eighth day), and *Δilp6* (no pupae at sixth day, 8% at seventh day, and 72% at eighth day) mosquitoes with smaller body size and depleted lipids. There were slight changes in the pupation rates of *Δilp4* (27% at sixth day and 84% at seventh day) compared with WT controls (11% at sixth day and 73% at seventh day) (Fig. 7*A* and *SI Appendix*, Fig. S6).

We determined the percentage of eclosed adults of *ΔAa5HT2B* and *ilp* (*Δilp2*, *Δilp6*, *Δilp5*, *Δilp4*) mutants. The mutants with diminished lipid reserves and small body sizes (*ΔAa5HT2B*, *Δilp2*, and *Δilp6*) exhibited significantly delayed eclosion and shorter lifespan, with no adults at the 8th day, only 5% (*ΔAa5HT2B*), 8% (*Δilp2*), and 10% (*Δilp6*) of adults at the 9th day from egg hatching, and the majority eclosed on the 11th day (Fig. 7 *B* and *C* and *SI Appendix*, Fig. S6). In contrast, 70% of

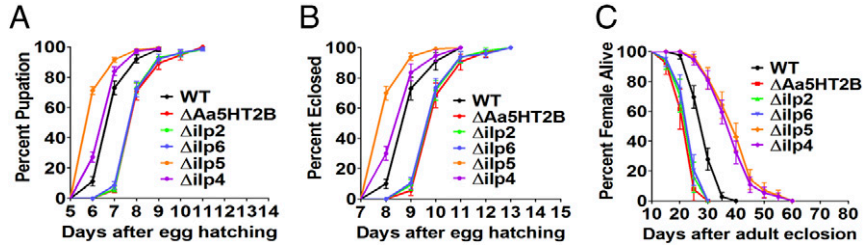

Fig. 7. Maturation time in WT control and mutant females. (*A*) The percentage of pupation. (*B*) The percentage of eclosion. (*C*) The percentage of live females shows the longevity. *ΔAa5HT2B* (red line), *Δilp2* (green line), and *Δilp6* (blue line) exhibit a delayed pupation and eclosion with a shorter lifespan; but *Δilp5* (yellow line) and *Δilp4* (purple line) exhibit a precocious pupation and eclosion with a longer lifespan than WT controls (black line). The log-rank test rests for the pupation curves and eclosion curves (times-to-event) are $P < 0.0001$; thus, the curves are significantly different.

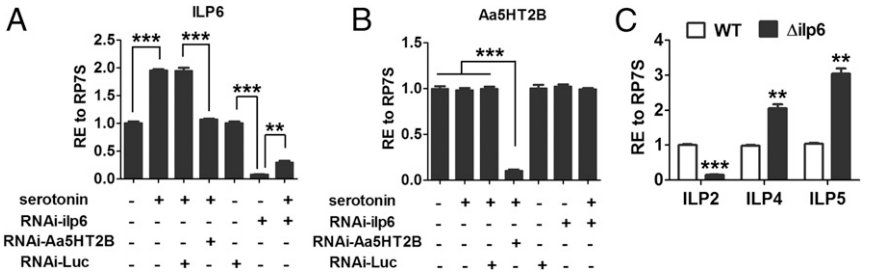

Fig. 8. ILP6 acts as an intermediate component of serotonin/Aa5HT2B-mediated *ilp* gene regulation. (*A*) Effects of serotonin and the serotonin receptor Aa5HT2B on the expression of the *ilp6* gene. Serotonin treatment increases the transcription of *ilp6*, whereas RNAi loss of Aa5HT2B renders the *ilp6* gene insensitive to serotonin. (*B*) Neither serotonin treatment nor RNAi depletion of ILP6 affects the transcription of *Aa5HT2B* gene. (*C*) Effects of CRISPR-Cas9 depletion of ILP6 on the transcription of the *ilp2*, *-4*, and *-5* genes derived from different tissues. Data of in vitro culture experiments represent 24 individuals in each replication with three technical replicates; data of in vivo tests represent three biological replicates (10 individuals in each replication) with three technical replicates. They are shown as mean ± SEM. $^{**}P < 0.01$; $^{***}P < 0.001$.

Δilp5 mutants with large body size and elevated lipid deposits eclosed at the eighth day and 94% at ninth day, compared with 10% (at eighth day) and 72% (at ninth day) of WT controls (Fig. 7*B* and *SI Appendix*, Fig. S6). Only 30% of *Δilp4* mutants, which had elevated lipid reserves and only slightly enlarged bodies, emerged on the eighth day (82% *Δilp4* at the ninth day) (Fig. 7*B* and *SI Appendix*, Fig. S6). *Δilp5* and *Δilp4* mutant females exhibited a longer lifespan, while *Δilp2* and *Δilp6* had a considerably shorter one than WT control (Fig. 7*C*). Taken together, these data demonstrate that maturation time and longevity depend not only on lipid nutrition reserves but also body size.

ILP6 Is a Possible Intermediate Component of the 5-HT/Aa5HT2B Regulatory Hierarchy to Control *ilp2*, *-4*, and *-5* Gene Expression. First, we dissected the fat-body from the abdominal wall; the quantitative real-time PCR analysis has shown that ILP6 originates from this tissue (*SI Appendix*, Fig. S7). We tested whether the fat-body–derived ILP6 mediates Aa5HT2B action. We carried out experiments combining RNAi silencing and an in vitro fat-body culture. Fat-bodies isolated from 72-h posteclosion female mosquitoes with RNAi-depleted *Luc*, *ILP6*, or *Aa5HT2B* were incubated in the presence or absence of serotonin. Serotonin increased transcript levels of *ilp6* gene in *Luc* RNAi mosquito fat-bodies, whereas *Aa5HT2B* RNAi depletion rendered ILP6 insensitive to serotonin signaling (Fig. 8*A*). ILP6 RNAi silencing or serotonin incubation had no effect on the expression of the *Aa5HT2B* gene (Fig. 8*B*). These experiments suggest that Aa5HT2B regulates *ilp6* expression in the fat-body. Next, we investigated the effect of CRISPR-Cas9 *ilp6* depletion on the expression of other *ilps*. The *ilp2* gene was down-regulated, while *ilp4* and *ilp5* were up-regulated in CRISPR-Cas9 *ilp6*-depleted female mosquitoes compared with WT controls (Fig. 8*C*). Taken together, these results have suggested that ILP6 is likely a factor downstream of Aa5HT2B that mediates control of ILP2, -4, and -5 derived from distinct tissues.

Phenotypic Rescue in CRISPR-Cas9 *Aa5HT2B*/*ilp5* Double-Knockout Mosquitoes. To investigate whether the Aa5HT2B-regulated *ilp* genes are the authentic trigger of the defects in growth and metabolism, we conducted phenotypic rescue experiments using CRISPR-Cas9 to generate the *Aa5HT2B*/*ilp5* double-knockout mosquitoes. First, we introduced the mixture of sgRNAs (40 ng/μL *Aa5HT2B*-sgRNA and 40 ng/μL *ilp5*-sgRNA) and Cas9 protein (333 ng/μL) into embryos (n = 2000). Of these embryos, 36% survived, reaching larval stage and adulthood, named Δ(*2B+ilp5*). Our DNA sequencing has shown the successful genomic mutations of both target genes (*SI Appendix*, Fig. S8*A*). To evaluate the impact of *Aa5HT2B-ilp5* CRISPR-Cas9 disruption on body size and metabolism, the Δ(*2B+ilp5*) mutants and WT control animals were raised and maintained under identical conditions at every stage of their development. We estimated the adult body sizes by measuring wing length and found that the Δ(*2B+ilp5*) mutants had only slightly longer wing length than WT females (Fig. 9*A*). We also observed recoveries of pupation/eclosion rates (Fig. 9 *B* and *C*), larval/pupal size (*SI Appendix*, Fig. S8 *B* and *C*), and wing cell size (*SI Appendix*, Fig. S8*D*). Next, we performed lipid droplet Nile red staining of the Δ(*2B+ilp5*)/WT females and examined TAG/glycogen levels in 24-h PBM adults and fifth-day fourth-instar larvae. The Δ(*2B+ilp5*) improved the nutrition status compared with WT control, *ΔAa5HT2B* and *Δilp5* (Fig. 10). In addition, we dissected the ovaries at 24-h PBM and found that *Aa5HT2B-ilp5* disruption partially rescued the ovarian development with *ΔAa5HT2B* (*SI Appendix*, Fig. S2*D*) and *Δilp5* mutants (*SI Appendix*, Fig. S5*B*). However, Δ(*2B+ilp5*) mutant females had less developed ovaries

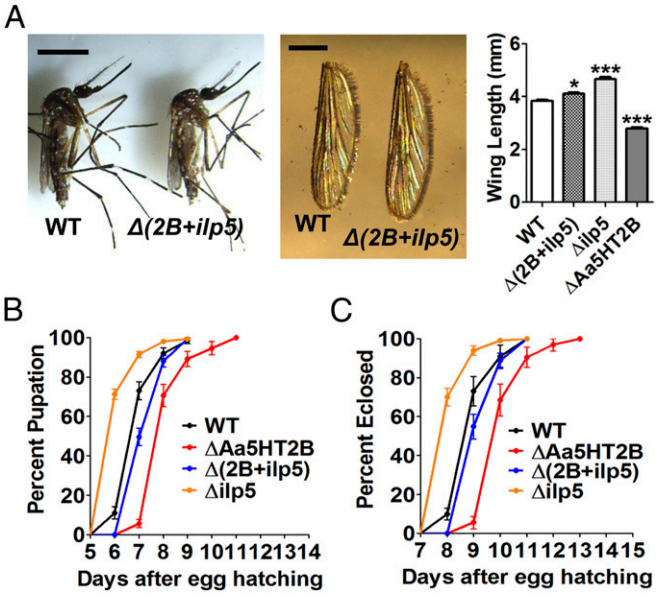

Fig. 9. Rescue of the Aa5HT2B-depletion phenotypes by CRISPR-Cas9 genomic disruption of ILP5. (*A*) Comparison of female body size (*Left*) and wing length (*Right*) between WT control and the *Δ(2B+ilp5)* mutants (compound knockout of *Aa5HT2B* and *ilp5* genes by CRISPR-Cas9). [Scale bars: 2 mm (*Left*) and 1 mm (*Right*).] All females (n = 285) were used for measurement. $^{*}P < 0.05$; $^{***}P < 0.001$. (*B* and *C*) Rescue of pupation (*B*) and eclosion (*C*) rates in double CRISPR-Cas9 depletion of *Aa5HT2B* and *ilp5*. The log-rank test rests for the pupation curves and eclosion curves (times-to-event) are $P < 0.0001$; thus, the curves are significantly different; 200 individuals in one culture container were used for counting.

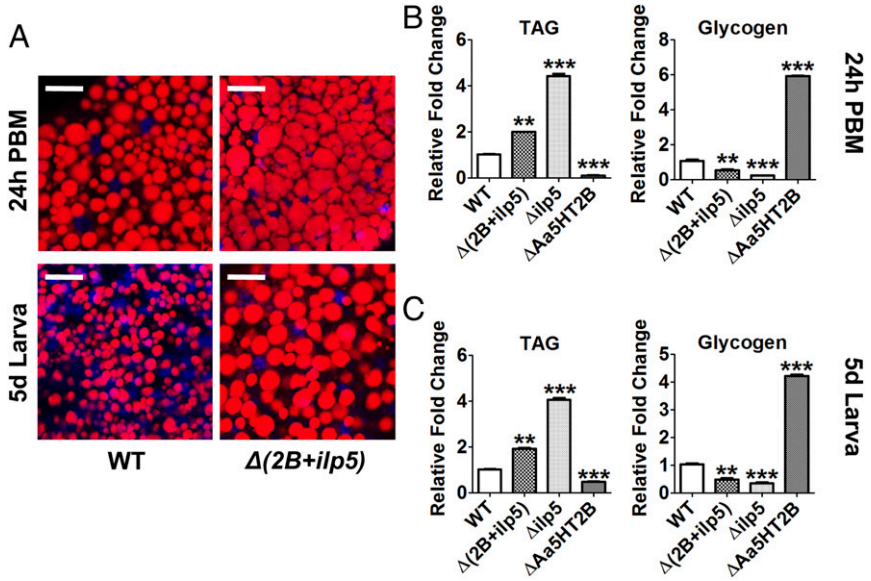

Fig. 10. Recovery of the nutrition status in double CRISPR-Cas9 depletion of *Aa5HT2B* and *ilp5*. (*A*) Lipid droplets in the fat-body dissected from adult females (24-h PBM) and larvae (fifth day after egg hatching) of WT and mutants were detected by Nile red and visualized under a confocal microscope (Scale bars, 25 μm.). Blue, DAPI staining. (*B* and *C*) The changes in TAG and glycogen levels in *Aa5HT2B-ilp5* CRISPR-Cas9 mutant adults (*B*) and fourth-instar larvae (*C*) were alleviated. Data represent three biological replicates (six individuals in each replication) with three technical replicates and are shown as mean ± SEM. $^{**}P < 0.01$; $^{***}P < 0.001$.

than in WT mosquitoes (*SI Appendix*, Fig. S8*E*, *Upper*). Their egg deposition was severely limited (*SI Appendix*, Fig. S8*E*, *Lower*). CRISPR-Cas9 depletion of *ilp5* appears to have no effect on the expression of *Aa5HT2B* or *ilp2*, *-4*, and *-6* (*SI Appendix*, Fig. S9).

Discussion

Evolution by natural selection has shaped organisms in two important ways, maximizing both metabolic capacity and the internal efficiency to sustain and reproduce life (25). An optimal species-specific body size is essential for other characteristics, such as metabolism, habitat, life history, and extinction risk (25). Control of body size is extremely complex and provided by numerous intrinsic and environmental cues (2). In this work, we have identified the fat-body–specific serotonin signaling that is involved in regulation of body size and metabolism in mosquitoes. Furthermore, the fat-body–specific serotonin receptor Aa5HT2B mediates this serotonin action. The fat-body is the main nutrient sensor in insects, linking nutritional state, metabolism, and growth (2, 19). In adult female mosquitoes, this tissue is central for coordinating the blood-meal–activated amino acid signaling with subsequent egg maturation (26). We found that a blood meal elevates the level of peripheral serotonin and Aa5HT2B, revealing another signaling adaptation of mosquitoes for hematophagy.

Insulin-like signaling is a conserved mechanism that coordinates growth and metabolism with nutrient status (4). Expression and release of ILPs are controlled by a number of means, including nutrients, steroid hormone, and neurotransmitters, such as serotonin (27). In *Drosophila*, serotonin that functions as a neurotransmitter in the brain regulates ILPs (27). *Drosophila* NS3 (a nucleostemin-family GTPase) acts on serotonergic neurons to control global growth by regulating DILP2 levels expressed in brain cells (24). Ablation of these IPCs in the *Drosophila* adult brain leads to increased storage of both lipid and carbohydrate (28). Knockdown of *Drosophila* brain-specific 5HT1A receptor in IPCs by RNAi leads to increased expression of *dilp2* and *dilp5* mRNA, decreased starvation resistance and food intake, but no effect on growth (29). DILP2 ubiquitous overexpression increases body size (30). Although the insect brain was shown to integrate peripheral metabolic information to direct feeding behavior and energy homeostasis, the mechanisms of serotonin in the insect fat-body and corresponding control of metabolism remained elusive.

Utilization of the CRISPR-Cas9 approach has permitted us to elucidate the role of Aa5HT2B in determination of body size and metabolic status in mosquitoes. A diminished lipid deposition and abnormal ovary development response to *Aa5HT2B* CRISPR-Cas9 disruption indicate participation of this serotonin receptor in regulation of metabolism and reproduction; in addition, decreased body size and postponed maturation led us to implicate insulin signaling in the serotonin receptor pathway in mosquitoes. We found that Aa5HT2B interacts with the insulin pathway affecting the transcription levels of *ilp2*, *-6*, *-5*, and *-4*. Interestingly, our experiments demonstrate that this serotonin receptor activates *ilp2* and *-6*, but represses *ilp4* and *-5*. Additional experiments were conducted to clarify the Aa5HT2B effects. Previously, DILP6 in *Drosophila* was characterized as the fat-body–secreted IGF (31). Riehle et al. (32) have found that the ILP6 transcript is enriched in the thorax and the abdominal wall of *A. aegypti* mosquito, suggesting its presence in the fat-body. Using isolated fat-bodies, we have shown that the mosquito ILP6 is specific to this tissue. Therefore, we utilized the in vitro fat-body culture combined with serotonin incubations and RNAi depletions to investigate the relationship between ILP6 and Aa5HT2B in this tissue. The results imply that serotonin activates ILP6 via Aa5HT2B, but ILP6 has no effect on *Aa5HT2B* expression. Serotonin levels are up-regulated in response to a blood meal, linking a nutritional signaling with *ilp6* activation. In contrast, starvation activates *dilp6* in both *Drosophila* larvae and adults (31, 33). Additional studies should clarify this difference in regulation of DILP6 and the mosquito ILP6. We further investigated the role of the fat-body–derived mosquito ILP6 and found that the CRISPR-Cas9 *ilp6* deletion affects the expression of *ilp2*, *-4*, and *-5*. This appears to suggest a regulatory link between ILP6 and other ILPs, in which ILP6 activates *ilp2* and represses *ilp4* and *-5*. Significantly, the simultaneous CRISPR-Cas9 loss of *Aa5HT2B* and *ilp5* rescued some phenotypic manifestations associated with either

DEVELOPMENTAL BIOLOGY

Aa5HT2B or *ilp5* deletions. In particular, the body size of these double mutants was nearly similar to that of WT mosquitoes. Equally, metabolic indicies, related to TAG and glycogen, were partially restored. This confirms the importance of Aa5HT2B and ILPs for body-size determination and metabolism homeostasis. However, fecundity of these mutants was still severely affected, showing that other factors are likely to be essential for reproductive events. Further studies are required to fully explain the mechanism underlying the rescue phenomenon in the Δ(*2B+ilp5*) mutants.

In insects, growth is mediated by ILPs acting through a canonical downstream kinase cascade (34). In *A. aegypti* mosquitoes, eight ILPs have been identified. In particular, *ilp1*, *ilp3*, and *ilp8* are expressed exclusively in heads as an operon; *ilp4* and *ilp7* are expressed in female heads; *ilp5* is expressed most abundantly in the abdominal body wall; and *ilp6* is the fat-body–derived IGF (31). We investigated the roles of ILP2, -4, -5, and -6 in the control of body size and metabolism homeostasis using the genetic CRISPR-Cas9 approach, and have shown that *ilp2* and *ilp6* CRISPR-Cas9–depleted mosquito mutants had smaller body sizes, while mosquitoes of the *ilp5*-depleted mutant exhibited a dramatically larger body size, suggesting that ILP2, -6, and -5 are involved in body size control. Additionally, lipid reserves were reduced in *ilp2*- and *ilp6*-depleted mutants, but elevated in *ilp5*- and *ilp4*-depleted mutants. Moreover, we observed that glycogen levels exhibited the opposite trends in these mutant mosquitoes, and ovarian development was affected, indicating that the antagonistic actions of ILP-2 and -6, and -5 and -4 are also involved in regulation of carbohydrate metabolism required for normal development and reproduction. We have previously reported CRISPR-Cas9 analysis of *ilp7* and *ilp8* and found that these two ILPs also exhibit opposite effects on lipid accumulation (35). However, body size was not affected in these CRISPR-Cas9 mutants. Further studies are required to elucidate the observed differences in ILP actions at the molecular level.

Both energy resources acquired for juvenile growth and the timing of feeding cessation during the final larval instar are critical to the final adult body-size determination (36, 37). Thus, we used the fifth-day fourth-instar larva when it stops feeding (wandering stage) as a checkpoint to determine the larval body size. We found that the mutant larvae displayed changes in body size the same as that seen in pupae and adults. Moreover, we used the fifth-day larvae to determine the levels of TAG and glycogen, and found similar changes to those observed in adulthood, indicating that a regulated balance between lipid and sugar metabolism during juvenile growth influences the final adult body size. How individuals determine the feeding and growth cessation is a larger question. Here, we identified that fat-body–specific 5-HT/Aa5HT2B signaling plays an essential role in controlling the timing of pupation and eclosion by regulating the balance of nutrition storage, which is a primary determinant of lifespan. Body size is controlled by insulin-like signaling and depends on nutrient use and cell growth (38). When we investigated the cell sizes in the wings of CRISPR-Cas9 mutants and WT control mosquitoes, we observed a strong correlation between their dimensions, body size, and lipid reserves. The cell size was reduced in *ΔAa5HT2B*, *Δilp2*, and *Δilp6*, but elevated in *Δilp5* to the same extent as the body-size mutation, indicating that the overall body-size phenotypes in these mutants are caused by the variations in cell size.

In conclusion, using the CRISPR-Cas9 gene-editing system and fat-body–specific GAL4-UAS RNAi, our study has uncovered the essential role of the fat-body–specific serotonin receptor Aa5HT2B in regulation of body size and metabolism in *A. aegypti*. *Aa5HT2B* CRISPR-Cas9 disruption decreased expression of *ilp2* and *-6* and antagonistically increased that of *ilp5* and *-4*. Functional evidence demonstrated that modulation of these ILPs by Aa5HT2B is required for control of growth and metabolism in mosquitoes. Further investigation using the CRISPR-Cas9 system has revealed differential roles of ILPs in these essential processes, especially the antagonistic actions of ILP5. We have also provided evidence that peripheral serotonin recruits the fat-body ILP6 via the Aa5HT2B receptor to transmit fat-body metabolic information and regulate *ilp2*, *ilp5*, and *ilp4* expression, thereby exerting control in body-size growth and metabolism homeostasis. Altogether, our results recognize Aa5HT2B as a fundamental element of the hitherto undefined fat-body–specific serotonin signaling system governing antagonistic ILP actions that ensures stability of development and plasticity of metabolism and body size.

Materials and Methods

Mosquito Rearing. *A. aegypti* larvae were reared at 27 °C in water supplemented with complete larval food (a mixture of rat chow, yeast, and lact-albumin, 1:1:1 ratio). Adult mosquitoes were reared at 27 °C and 80% humidity with unlimited access to water and 10% (wt/vol) sucrose solution. Four-day-old females were blood-fed on White Leghorn chickens. The use of vertebrate animals was approved by the University of California Riverside Institutional Animal Care and Use Committee.

Determination of Serotonin Levels. Serotonin levels were measured using the serotonin ELISA kit (ImmuSmol). In brief, 30 mosquito heads or bodies were used per assay and homogenized in Diluent Buffer (Invitrogen). The supernatant was subjected to acylation and quantification according to the manufacturer's instructions.

RNA Extraction and Quantitative Real-Time PCR. Total RNA was extracted using TRIzol (Invitrogen); cDNAs were produced using the SuperScript III Reverse Transcriptase (Invitrogen); and quantitative real-time PCR was performed using the SYBR Green Supermix (Bio-Rad), all according to the manufacturer's instructions. Each sample was measured in triplicate, and relative expression was calculated as $2^{-\Delta\Delta Ct}$ and normalized with the housekeeping gene *RPS7*.

Embryonic Injection for CRISPR-Cas9. sgRNAs were synthesized using the MEGAscript T7 Transcription Kit (Ambion) (*SI Appendix*, Table S1) and purified using the MEGAclear Transcription Clean-Up Kit (Ambion) following the manufacturer's instructions. Next, 40 ng/μL sgRNAs and 333 ng/μL Cas9 protein (PNA Bio) were microinjected into preblastoderm embryos in the posterior pole. The injected eggs were hatched on the fifth day after injection and reared to adulthood.

Generating Transgenic Mosquitoes. Fat-body–specific RNAi was generated by the transgenic mosquitoes *Vg-Gal4/UAS-iAa5HT2B*. The driver *Vg-Gal4* line was generated previously (23). The responder line *UAS-iAa5HT2B* was produced by microinjecting transformation vector pBac[3xP3-DsRed, UAS-iAa5HT2B] and helper into preblastoderm embryos from the posterior pole. The UAS-iAa5HT2B fragments containing a fold-back construct of the double-stranded *Aa5HT2B* RNA (iAa5HT2B) were inserted into the pBac[3xP3-DsRed] plasmid at the AscI restriction site. The iAa5HT2B construct consists of a sense 498-pb fragment from the *Aa5HT2B* coding sequence (*SI Appendix*, Table S1), followed by a spacer and antisense conformation of this fragment (39). Germline transformation was performed according to described protocols (23).

Immunoblot. Protein analyses of LP (Lipophorin) and VG (Vitellogenin) were performed by means of Western blot. The lysates from blood-fed females were loaded with 2× Laemmli Sample Buffer (Sigma) on 4–20% protein gels (Bio-Rad) and transferred to PVDF membranes in the NuPAGE Transfer Buffer (Thermo Fisher) and 20% (vol/vol) methanol. The membranes were blocked in StartingBlock (PBS) Buffer (Thermo Fisher). For VG detection, the VG antibody (1:5,000 dilution) was used followed by the secondary anti-mouse–HRP (Abcam) at a 1:5,000 dilution. For LP detection, apolipoprotein-I polyclonal antibody (1:10,000 dilution) was used followed by the secondary anti-rabbit–HRP (Abcam) at a 1:5,000 dilution. Monoclonal antibody for β-actin (Sigma) was used as a loading control.

Lipid Droplet Staining. Fat-bodies were incubated in Nile red solution (20% glycerol in PBS, with a 1:10,000 dilution of 10% Nile red in DMSO), mounted by ProLong Diamond Antifade Mountant with DAPI (Thermo Fisher) and examined under a Leica SP5 confocal laser-scanning microscope.

Determination of TAG Levels. TAG levels were measured using the Triglyceride Colorimetric Assay (Cayman) following the manufacturer's instructions. Six

mosquitoes were homogenized in 100 μL of Diluent Assay Reagent (Cayman). Then, 10 μL of the supernatant was incubated with enzyme (Cayman). The values of TAG contents were measured and results were calculated using the equation obtained from the standard curve.

Determination of Glycogen Levels. Glycogen levels were measured using the Glycogen Assay Kit (Cayman) following the manufacturer's instructions. Six fat-bodies were homogenized in 100 μL of Diluent Assay Buffer (Cayman). A 10-μL sample of supernatant was incubated with enzyme (Cayman). The values of glycogen contents were measured and results were calculated using the equation obtained from the standard curve.

Analysis of Body Size and Cell Size. Adult body size was estimated by adult wing length measurement. Larval body size was determined on fifth-day last-instar larvae (wandering fourth-instar larval stage) by the linear measurement of body length between the initial vertex of head capsule and terminal vertex of abdominal segments. Wings from WT controls and mutant females were visualized under a Leica SP5 confocal microscope, and mean cell area was measured by counting the number of wing hairs within 45 × 45-μm squares ($n = 20$) in the area between two defined wing veins. Cell size in the wings was calculated by dividing the square area by the number of wing hairs.

In Vitro Fat-Body Culture. Fat-bodies from 3-d-old females were incubated in the complete medium with or without serotonin (Sigma). Three fat-bodies were incubated in each well (96-well plates) with a complete medium, as previously described (40). For serotonin treatment, 5 μM serotonin was added to the culture medium. All incubations lasted 6 h, after which samples were collected for quantitative real-time PCR analysis. Data represent 24 individuals in each replication with three technical replicates.

Phylogenetic Tree Construct. Alignments and phylogenetic tree construct were performed with MEGA7 by using the amino acid sequence of ORF. Maximum-likelihood analysis was calculated with MEGA7 (21).

Statistical Analysis. All statistical values are presented as mean ± SEM. Mean values were compared using the Student's *t* test at the following significance levels: $*P < 0.05$, $**P < 0.01$, and $***P < 0.001$. Statistical analyses were performed using GraphPad Prism 6.

ACKNOWLEDGMENTS. We thank Drs. Naoki Yamanaka and Naoki Okamoto for making constructive suggestions. This work was supported by NIH Award 2R01AI036959 (to A.S.R.).

1. Attardo GM, Hansen IA, Raikhel AS (2005) Nutritional regulation of vitellogenesis in mosquitoes: Implications for anautogeny. *Insect Biochem Mol Biol* 35:661–675.
2. Boulan L, Milán M, Léopold P (2015) The systemic control of growth. *Cold Spring Harb Perspect Biol* 7:a019117.
3. Nijhout HF, et al. (2014) The developmental control of size in insects. *Wiley Interdiscip Rev Dev Biol* 3:113–134.
4. Tennessen JM, Thummel CS (2011) Coordinating growth and maturation—Insights from *Drosophila*. *Curr Biol* 21:R750–R757.
5. Colombani J, Andersen DS, Léopold P (2012) Secreted peptide Dilp8 coordinates *Drosophila* tissue growth with developmental timing. *Science* 336:582–585.
6. Garelli A, Gontijo AM, Miguela V, Caparros E, Dominguez M (2012) Imaginal discs secrete insulin-like peptide 8 to mediate plasticity of growth and maturation. *Science* 336:579–582.
7. Rulifson EJ, Kim SK, Nusse R (2002) Ablation of insulin-producing neurons in flies: Growth and diabetic phenotypes. *Science* 296:1118–1120.
8. Jünger MA, et al. (2003) The *Drosophila* forkhead transcription factor FOXO mediates the reduction in cell number associated with reduced insulin signaling. *J Biol* 2:20.
9. Rintelen F, Stocker H, Thomas G, Hafen E (2001) PDK1 regulates growth through Akt and S6K in *Drosophila*. *Proc Natl Acad Sci USA* 98:15020–15025.
10. Verdu J, Buratovich MA, Wilder EL, Birnbaum MJ (1999) Cell-autonomous regulation of cell and organ growth in *Drosophila* by Akt/PKB. *Nat Cell Biol* 1:500–506.
11. Ramnanan CJ, et al. (2013) Interaction between the central and peripheral effects of insulin in controlling hepatic glucose metabolism in the conscious dog. *Diabetes* 62:74–84.
12. Wang X, et al. (2017) Hormone and receptor interplay in the regulation of mosquito lipid metabolism. *Proc Natl Acad Sci USA* 114:E2709–E2718.
13. El-Merahbi R, Löffler M, Mayer A, Sumara G (2015) The roles of peripheral serotonin in metabolic homeostasis. *FEBS Lett* 589:1728–1734.
14. Novak MG, Ribeiro JMC, Hildebrand JG (1995) 5-hydroxytryptamine in the salivary glands of adult female Aedes aegypti and its role in regulation of salivation. *J Exp Biol* 198:167–174.
15. Pietrantonio PV, Jagge C, McDowell C (2001) Cloning and expression analysis of a 5HT7-like serotonin receptor cDNA from mosquito *Aedes aegypti* female excretory and respiratory systems. *Insect Mol Biol* 10:357–369.
16. Blenau W, Thamm M (2011) Distribution of serotonin (5-HT) and its receptors in the insect brain with focus on the mushroom bodies: Lessons from *Drosophila melanogaster* and *Apis mellifera*. *Arthropod Struct Dev* 40:381–394.
17. Pytliak M, Vargová V, Mechírová V, Felsöci M (2011) Serotonin receptors—From molecular biology to clinical applications. *Physiol Res* 60:15–25.
18. Arrese EL, Soulages JL (2010) Insect fat body: Energy, metabolism, and regulation. *Annu Rev Entomol* 55:207–225.
19. Colombani J, et al. (2003) A nutrient sensor mechanism controls *Drosophila* growth. *Cell* 114:739–749.
20. Briegel H (1985) Mosquito reproduction—Incomplete utilization of the blood meal protein for oogenesis. *J Insect Physiol* 31:15–21.
21. Kumar S, Stecher G, Tamura K (2016) MEGA7: Molecular Evolutionary Genetics Analysis version 7.0 for bigger datasets. *Mol Biol Evol* 33:1870–1874.
22. Nijhout HF, Callier V (2015) Developmental mechanisms of body size and wing-body scaling in insects. *Annu Rev Entomol* 60:141–156.
23. Kokoza VA, Raikhel AS (2011) Targeted gene expression in the transgenic *Aedes aegypti* using the binary Gal4-UAS system. *Insect Biochem Mol Biol* 41:637–644.
24. Kaplan DD, Zimmermann G, Suyama K, Meyer T, Scott MP (2008) A nucleostemin family GTPase, NS3, acts in serotonergic neurons to regulate insulin signaling and control body size. *Genes Dev* 22:1877–1893.
25. Clauset A, Erwin DH (2008) The evolution and distribution of species body size. *Science* 321:399–401.
26. Hansen IA, Attardo GM, Park JH, Peng Q, Raikhel AS (2004) Target of rapamycin-mediated amino acid signaling in mosquito anautogeny. *Proc Natl Acad Sci USA* 101:10626–10631.
27. Nässel DR, Vanden Broeck J (2016) Insulin/IGF signaling in *Drosophila* and other insects: Factors that regulate production, release and post-release action of the insulin-like peptides. *Cell Mol Life Sci* 73:271–290.
28. Broughton SJ, et al. (2005) Longer lifespan, altered metabolism, and stress resistance in *Drosophila* from ablation of cells making insulin-like ligands. *Proc Natl Acad Sci USA* 102:3105–3110.
29. Luo J, Becnel J, Nichols CD, Nässel DR (2012) Insulin-producing cells in the brain of adult *Drosophila* are regulated by the serotonin 5-HT1A receptor. *Cell Mol Life Sci* 69:471–484.
30. Brogiolo W, et al. (2001) An evolutionarily conserved function of the *Drosophila* insulin receptor and insulin-like peptides in growth control. *Curr Biol* 11:213–221.
31. Okamoto N, et al. (2009) A fat body-derived IGF-like peptide regulates postfeeding growth in *Drosophila*. *Dev Cell* 17:885–891.
32. Riehle MA, Fan Y, Cao C, Brown MR (2006) Molecular characterization of insulin-like peptides in the yellow fever mosquito, *Aedes aegypti*: Expression, cellular localization, and phylogeny. *Peptides* 27:2547–2560.
33. Umezaki Y, et al. (2018) Feeding-state-dependent modulation of temperature preference requires insulin signaling in *Drosophila* warm-sensing neurons. *Curr Biol* 28:779–787.e3.
34. Garofalo RS (2002) Genetic analysis of insulin signaling in *Drosophila*. *Trends Endocrinol Metab* 13:156–162.
35. Ling L, Kokoza VA, Zhang C, Aksoy E, Raikhel AS (2017) MicroRNA-277 targets *insulin-like peptides 7* and *8* to control lipid metabolism and reproduction in *Aedes aegypti* mosquitoes. *Proc Natl Acad Sci USA* 114:E8017–E8024.
36. Lee GJ, et al. (2018) Steroid signaling mediates nutritional regulation of juvenile body growth via IGF-binding protein in *Drosophila*. *Proc Natl Acad Sci USA* 115:5992–5997.
37. Wegman LJ, Ainsley JA, Johnson WA (2010) Developmental timing of a sensory-mediated larval surfacing behavior correlates with cessation of feeding and determination of final adult size. *Dev Biol* 345:170–179.
38. Edgar BA (2006) How flies get their size: Genetics meets physiology. *Nat Rev Genet* 7:907–916.
39. Bian G, Shin SW, Cheon HM, Kokoza V, Raikhel AS (2005) Transgenic alteration of Toll immune pathway in the female mosquito *Aedes aegypti*. *Proc Natl Acad Sci USA* 102:13568–13573.
40. Saha TT, et al. (2016) Hairy and Groucho mediate the action of juvenile hormone receptor methoprene-tolerant in gene repression. *Proc Natl Acad Sci USA* 113:E735–E743.